Tensor-Based Morphometry with Mappings Parameterized by Stationary Velocity Fields in Alzheimer's Disease Neuroimaging Initiative

Matías Nicolás Bossa, Ernesto Zacur, and Salvador Olmos

GTC, Aragon Institute of Engineering Research (I3A), University of Zaragoza, Spain
{bossa,zacur,olmos}@unizar.es

Abstract. Tensor-based morphometry (TBM) is an analysis technique where anatomical information is characterized by means of the spatial transformations between a customized template and observed images. Therefore, accurate inter-subject non-rigid registration is an essential prerequisite. Further statistical analysis of the spatial transformations is used to highlight some useful information, such as local statistical differences among populations. With the new advent of recent and powerful non-rigid registration algorithms based on the large deformation paradigm, TBM is being increasingly used. In this work we evaluate the statistical power of TBM using stationary velocity field diffeomorphic registration in a large population of subjects from Alzheimer's Disease Neuroimaging Initiative project. The proposed methodology provided atrophy maps with very detailed anatomical resolution and with a high significance compared with results published recently on the same data set.

1 Introduction

Alzheimer's disease (AD) is the most common form of dementia and one of the most serious health problems in the industrialised world. Dementia affects approximately 1–5% of the population over 65 years of age, and 20–40% of the population over 80 years of age. Mild cognitive impairments (MCI) may affect 10 times as many individuals.

The Alzheimer's Disease Neuroimaging Initiative (ADNI) [1] is a large multi-site longitudinal magnetic resonance imaging (MRI) and fluorodeoxyglucose positron emission tomography (FDG-PET) study of 800 adults, ages 55 to 90, including 200 elderly controls, 400 subjects with mild cognitive impairment, and 200 patients with AD. The primary goal of ADNI has been to test whether serial MRI, PET, other biological markers, and clinical and neuropsychological assessment can be combined to measure the progression of MCI and early AD. Determination of sensitive and specific markers of very early AD progression is intended to aid researchers and clinicians to develop new treatments and monitor their effectiveness, as well as lessen the time and cost of clinical trials.

Tensor-based morphometry (TBM) is a relatively new image analysis technique that identifies regional structural differences in the brain, across groups

or over time, from the gradients of the deformation fields that warp images to a common anatomical template. The anatomical information is encoded in the spatial transformation. Therefore, accurate inter-subject non-rigid registration is an essential tool. With the new advent of recent and powerful non-rigid registration algorithms based on the large deformation paradigm, TBM is being increasingly used [2,3,4]. Further statistical analysis of the spatial transformations is used to highlight some useful information, such as local statistical differences among populations. The simplest and most common feature is given by the Jacobian determinant $|J|$ which can be interpreted as a local atrophy/expansion factor. More complete descriptors are the Jacobian matrix, or other invariant features, such as $\sqrt{J^T J}$ [2].

By diffeomorphic registration we mean algorithms where the transformation can be arbitrarily large, and still keeping smoothness and invertibility. Most of these methods use time-varying velocity fields either to update or to characterize the warpings. The first approach was based on viscous-fluid methods [5]. Later, regularization was obtained by minimizing the length of a path on the group of diffeomorphisms [6]. Among the benefits of the latter approach is that its parametrization lives in a metric linear space allowing statistical analysis. The main limitation of these methods is their large computational complexity. In order to alleviate this computational requirement some algorithms were proposed [7,8,9] using a stationary velocity field parameterization.

The aim of this study was to evaluate the performance of stationary velocity field (SVF) diffeomorphic registration on a TBM study.

2   Materials and Methods

2.1   Subjects

In this study we selected the same subset of subjects as in [10] in order to allow an easier comparison. To summarize, MRI screening scans of 120 subjects, divided into 3 groups: 40 healthy elderly individuals, 40 individuals with amnestic MCI, and 40 individuals with probable AD. Each group of 40 subjects was well matched in terms of gender and age. Likewise [10], an independent second group of normal subjects, age- and gender-matched to the first group of controls, was selected to test whether analysis techniques correctly detects no differences when no true differences are present. More details about criteria for patient selection and exclusion can be found in [10] and in the ADNI protocol [1,11].

In addition, a larger set of subjects was analyzed including 231 control subjects, 200 AD patients and 405 MCI patients from the ADNI study at screening stage. During the clinical follow up 127 MCI subjects converted to AD group. The MCI group was divided into converters (MCIc) and non-converters (MCInc).

2.2   MRI Acquisition, Image Correction and Preprocessing

High-resolution structural brain MRI scans were acquired at multiple ADNI sites using 1.5 Tesla MRI scanners using the standard ADNI MRI protocol.

For each subject, two T1-weighted MRI scans were collected using a sagittal 3DMP-RAGE sequence with voxel size of $0.94 \times 0.94 \times 1.2mm^3$. The images were calibrated with phantom-based geometric corrections to ensure consistency among scans acquired at different sites Additional image corrections included geometric distortion correction, bias field correction and geometrical scaling. The pre-processed images are available to the scientific community and were downloaded from the ADNI website.

2.3   Stationary Velocity Fields (SVF) Diffeomorphic Registration

A diffeomorphism $\varphi(x)$ (smooth and invertible mapping) characterized by a stationary velocity field v is obtained as the solution at time $t = 1$ of

$$\frac{d}{dt}\phi_t(x) = v(\phi_t(x)), \qquad \phi_0(x) = Id(x), \tag{1}$$

i.e. $\varphi(x) \equiv \phi_1(x)$ and $v(x)$ is a smooth vector field. Several efficient numerical scheemes can be used to compute the exponential mapping $\exp(tv) \equiv \phi_t$ [12]. Note that the inverse mapping is $\varphi^{-1} = \phi_{-1} = \exp(-v)$.

Many registration methods can be formulated as a variational problem, where the cost function to be minimized contains an image term measuring matching between a template T and a target image I and a regularization term

$$E(I, T, v) = \frac{1}{\sigma^2}\|T(\varphi^{-1}) - I\|^2 + \langle v, v \rangle_V. \tag{2}$$

In this work the regularization term is of the form: $\langle v, v \rangle_V = \langle Hv, v \rangle_{L^2}$, with H the linear differential operator $H = (Id - \alpha\triangle)^2$, where $\triangle$ is the Laplacian operator. The gradient of this functional is (see [6])

$$\nabla_v E(I, T, v) = 2v - \frac{2}{\sigma^2}H^{-1}\int_0^1 |D\phi_{1-t}|\big(T(\phi_{-t}) - I(\phi_{1-t})\big)\nabla_x T(\phi_{-t})dt \tag{3}$$

Different strategies have been proposed to minimize the energy functional defined by (2) [13,8,7,9]. In [7] the derivative of $\exp(v)$ was appoximated by $\partial_h \exp(v) \approx h$ for $v \approx 0$, resulting in a simplified gradient $\nabla_v E(I, T, v) = 2v - \frac{2}{\sigma^2}H^{-1}\big((T(\phi_{-1}) - I)\nabla_x T(\phi_{-1})\big)$ which reduces significatively the computational complexity when using gradient descent.

2.4   Unbiased Average Template

An average template is one of the key components of TBM studies. It provides a coordinate system where all image samples will be registered. In order to make automatic registration easier and more robust, the template must represent common intensity and geometric features from the group of subjects. Population templates should not be biased toward any particular image or sub-group of images.

In this work the unbiased template T was estimated from images of the normal group, likewise in [10]. An initial affine average atlas was estimated by means of global affine registration of all intensity-normalized normal group images I^i to the ICBM53 template and voxel-wise averaging. Next, an iterative process was used to estimate the template, including three stages for each iteration: non-linear registration of the affine-alligned images ($N = 40$) to the current estimated template; computing the bi-invariant mean $\overline{\varphi} = \exp(\overline{v})$ [14] of all warpings $\varphi^i = \exp(v^i)$, and finally image intensities are averaged after subtracting the mean warping $T = 1/N \sum_i I^i(\varphi^i \circ \exp(-\overline{v}))$.

2.5   Voxel-Wise Statistical Analysis of Brain Atrophy

To quantify spatial distribution of brain atrophy in MCI and AD compared to the normal group, all individual brains were non-linearly registered to the normal group template. Hypothesis testing is usually performed on logarithm of Jacobian determinants to assess effect size and statistical significance of local brain atrophy between patient groups. Statistical maps that visualize the patterns of significant expansion factors between groups were computed by means of t-test.

2.6   Regions of Interest Statistical Analysis

In order to summarize the information of hypothesis testing from the voxel level to the region of interest (ROI) level, a scalar descriptor of the ROI, such as a weighted average, the maximum value or many others, can be used. Similarly to [10], we used the average Jacobian determinant, which is equivalent to the
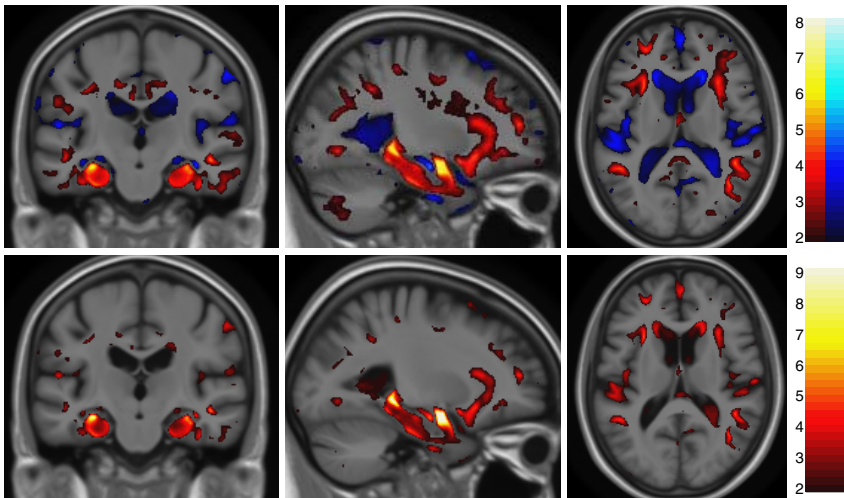

Fig. 1. Statistical maps of brain atrophy in the selected population ($N=120$) of AD versus Normal group. Top: Student's t-test map (blue/red denotes expansion/contraction respectively. Bottom: corresponding significance map ($-log_{10}\ p$).
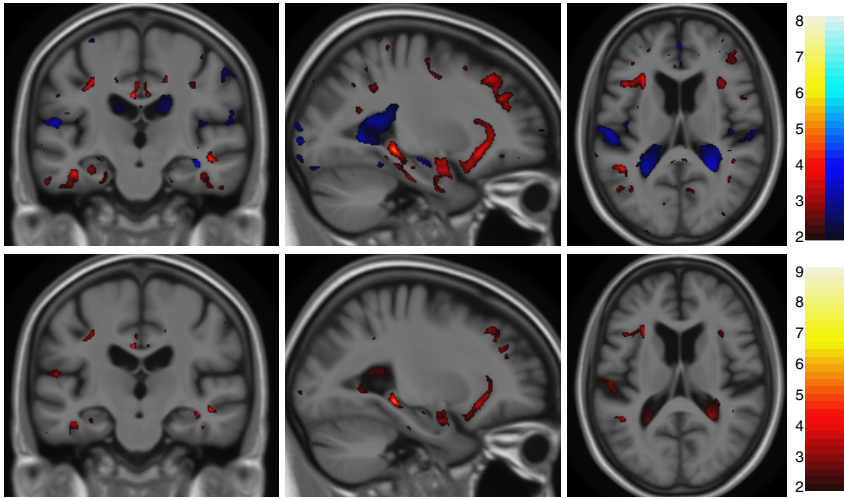
Fig. 2. Statistical maps of brain atrophy in the selected population (*N=120*) of MCI versus Normal group. See legend of Fig. 1.

overall volume change of the ROI. In this work the following ROIs were considered: hippocampus, amygdala, caudate nucleus, thalamus, nucleus accumbens and lateral ventricles. These subcortical nuclei were automatically segmented at the normal template using the tool FIRST [15] from FSL package.

3   Results

The statistical significance (*p*-value) and Student's t-test maps in Fig. 1(2) illustrate the atrophy pattern observed in the AD(MCI) groups compared to the normal group. AD patients showed larger areas affected by more severe brain atrophy specially at the hippocampus and amygdala. In contrast, brain atrophy in MCI patients affects smaller regions with a less pronounced effect size. Note that detected areas have a well defined anatomical boundary compared to previous results using the same data set [10]. The statistical map under the null hypothesis (between the two independent normal groups) did not show any significant region.

Table 1. ROI analysis: Student's t-test on large population (*N=836*)

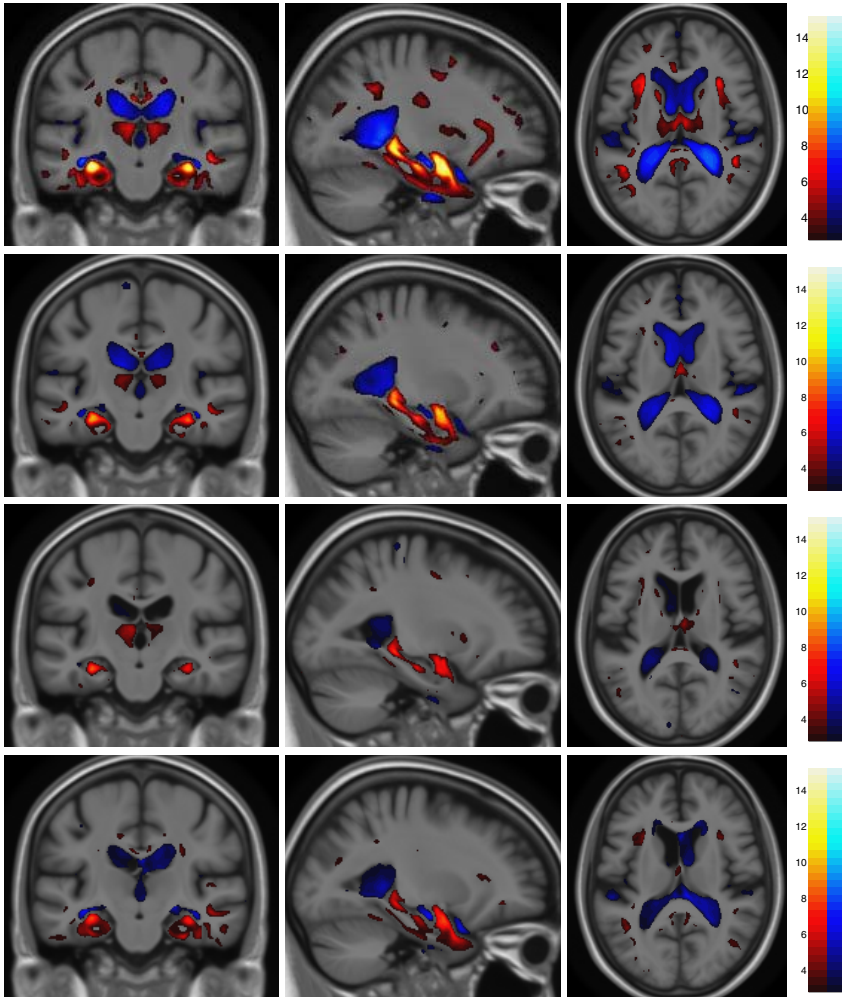| Groups\ROI	LAccu	LAmyg	LHipp	LLate	LThal	RAccu	RAmyg	RHipp	RLate	RThal
Nor vs AD	4.07	13.84	6.47	-6.48	4.68	4.17	13.57	9.66	-7.07	5.21
Nor vs MCIc	2.69	10.16	5.40	-5.12	3.68	2.54	8.98	6.96	-5.13	3.77
Nor vs MCInc	2.86	6.59	4.88	-3.49	3.69	2.45	5.78	6.07	-2.86	3.91
AD vs MCIc	-0.81	-2.29	-0.42	0.86	-0.45	-1.00	-2.58	-1.27	1.40	-0.55
AD vs MCInc	-1.44	-7.65	-2.18	3.15	-1.41	-1.98	-8.13	-4.26	4.38	-1.71
MCI c vs nc	-0.39	-4.31	-1.44	1.89	-0.76	-0.62	-4.16	-2.21	2.43	-0.83

Fig. 3. Student's t-test maps of brain atrophy in the large population (*N=836*). From top to bottom: AD versus Normal group; converter MCI versus Normal group; non-converter MCI versus Normal group; AD vs non-converter MCI group.

If the TBM analysis is performed on the larger population (N=836), very similar anatomical patterns of atrophy are obtained (see Fig. 3) but with a much higher statistical significance due to the larger number of subjects in the analysis. Interestingly, the brain atrophy map in the MCInc group was closer to the normal group, while the MCIc group was closer to the AD group.

The Jacobian determinant was spatially averaged within each ROI and subject. Student's t-test was performed on these scalar descriptors to assess the statistical significance between mean atrophy levels. Table 1 contains the Student's t-test statistic for each ROI on the complete set of subjects (*N=836*).

Again hippocampus and amygdala obtained the most significant volumetric differences between groups, in agreement with previous studies.

4   Discussion and Conclusions

In this study a large deformation registration method was used in a cross-sectional TBM study in order to localize brain atrophy regions in Alzheimer's disease and mild cognitive impairment patients. Compared to a recent TBM study with the same data set of 120 images at baseline from ADNI [10], our brain atrophy patterns presented a higher spatial resolution with a larger statistical significance. In our opinion, the improved performance obtained in this work may be due to the higher spatial resolution of the registration algorithm.

The evaluation was also extended to 836 subjects from ADNI corroborating brain atrophy patterns shown in the subset of subjects with stronger significance. Interestingly, brain atrophy patterns between converters and non-converters sub-groups of MCI compared to the normal group were very different. In particular, non-converters were much close to normal group, while converters were much closer to AD group. Our first preliminary results found brain atrophy at amygdala, hippocampus, entorhinal cortex, cingulate gyrus, posterior parts of the thalamus, frontal regions of the insular cortex, and superior temporal sulcus, all of them involved in Alzheimer's Disease. To our knowledge, this is the first time that all these structures are jointly identified in a brain morphometry study with such anatomical detail.

In future studies correlation between image-driven atrophy measurements and clinical variables (including cognitive tests, genotypes and biomarkers) will be assessed as it is proposed in [16], prediction of conversion to AD, single-subject analysis and evaluation of atrophy rates using longitudinal images.

References

1. Mueller, S.G., Weiner, M.W., Thal, L.J., Petersen, R.C., Jack, C., Jagust, W., Trojanowski, J.Q., Toga, A.W., Beckett, L.: The Alzheimer's Disease Neuroimaging Initiative. Neuroimaging Clinics of North America 15(4), 869–877 (2005)
2. Lepore, N., Brun, C., Chou, Y.Y., Chiang, M.C., Dutton, R., Hayashi, K., Luders, E., Lopez, O., Aizenstein, H., Toga, A., Becker, J., Thompson, P.: Generalized Tensor-Based Morphometry of HIV/AIDS Using Multivariate Statistics on Deformation Tensors. IEEE Transactions on Medical Imaging 27(1), 129–141 (2008)

3. Chiang, M.C., Dutton, R.A., Hayashi, K.M., Lopez, O.L., Aizenstein, H.J., Toga, A.W., Becker, J.T., Thompson, P.M.: 3D pattern of brain atrophy in HIV/AIDS visualized using tensor-based morphometry. NeuroImage 34(1), 44–60 (2007)

4. Lee, A.D., Leow, A.D., Lu, A., Reiss, A.L., Hall, S., Chiang, M.C., Toga, A.W., Thompson, P.M.: 3D pattern of brain abnormalities in Fragile X syndrome visualized using tensor-based morphometry. NeuroImage 34(3), 924–938 (2007)

5. Christensen, G., Rabbitt, R., Miller, M.: Deformable templates using large deformation kinematics. IEEE Transactions on Image Processing 5(10), 1435–1447 (1996)

6. Beg, M.F., Miller, M.I., Trouve, A., Younes, L.: Computing Large Deformation Metric Mappings via Geodesic Flows of Diffeomorphisms. International Journal of Computer Vision 61(2), 139–157 (2005)

7. Hernandez, M., Bossa, M., Olmos, S.: Registration of Anatomical Images Using Paths of Diffeomorphisms Parameterized with Stationary Vector Fields Flows. International Journal of Computer Vision (2009)

8. Ashburner, J.: A fast diffeomorphic image registration algorithm. NeuroImage 38(1), 95–113 (2007)

9. Vercauteren, T., Pennec, X., Perchant, A., Ayache, N.: Symmetric log-domain diffeomorphic registration: A demons-based approach. In: Metaxas, D., Axel, L., Fichtinger, G., Székely, G. (eds.) MICCAI 2008, Part I. LNCS, vol. 5241, pp. 754–761. Springer, Heidelberg (2008)

10. Hua, X., Leow, A.D., Lee, S., Klunder, A.D., Toga, A.W., Lepore, N., Chou, Y.Y., Brun, C., Chiang, M.C., Barysheva, M., Jack Jr., C.R., Bernstein, M.A., Britson, P.J., Ward, C.P., Whitwell, J.L., Borowski, B., Fleisher, A.S., Fox, N.C., Boyes, R.G., Barnes, J., Harvey, D., Kornak, J., Schuff, N., Boreta, L., Alexander, G.E., Weiner, M.W., Thompson, P.M., The Alzheimer's Disease Neuroimaging Initiative: 3D characterization of brain atrophy in Alzheimer's disease and mild cognitive impairment using tensor-based morphometry. NeuroImage 41(1), 19–34 (2008)

11. Mueller, S.G., Weiner, M.W., Thal, L.J., Petersen, R.C., Jack, C.R., Jagust, W., Trojanowski, J.Q., Toga, A.W., Beckett, L.: Ways toward an early diagnosis in Alzheimer's disease: The Alzheimer's Disease Neuroimaging Initiative (ADNI). Alzheimers Dement 1(1), 55–66 (2005)

12. Bossa, M., Zacur, E., Olmos, S.: Algorithms for computing the group exponential of diffeomorphisms: Performance evaluation. In: Proc. IEEE Computer Society Conference on Computer Vision and Pattern Recognition (CVPR), June 23-28, pp. 1–8 (2008)

13. Hernandez, M., Olmos, S.: Gauss-Newton optimization in Diffeomorphic registration. In: Proc. 5th IEEE International Symposium on Biomedical Imaging (ISBI), May 14-17, pp. 1083–1086 (2008)

14. Arsigny, V.: Processing Data in Lie Groups: An Algebraic Approach. Application to Non-Linear Registration and Diffusion Tensor MRI. PhD Thesis, École polytechnique (November 2006)

15. Patenaude, B.: Bayesian Statistical Models of Shape and Appearance for Subcortical Brain Segmentation. PhD thesis, University of Oxford (2007)

16. Hua, X., Leow, A.D., Parikshak, N., Lee, S., Chiang, M.C., Toga, A.W., Jack Jr., C.R., Weiner, M.W., Thompson, P.M.: Tensor-based morphometry as a neuroimaging biomarker for Alzheimer's disease: An MRI study of 676 AD, MCI, and normal subjects. NeuroImage 43(3), 458–469 (2008)